A mechanical Chua's circuit

A Mechanical Chua's Circuit: Feasible Or Not?

Thijs Verhees

DCT 2004.66

Traineeship report

Coach: L. Kodde

Supervisor: H. Nijmeijer

Technische Universiteit Eindhoven
Department Of Mechanical Engineering
Dynamics and Control Technology Group

Eindhoven, June, 2004

Contents

1 Introduction **1**

2 Chua's Circuit **2**
2.1 Governing Equations 2
2.2 Equilibrium Points 2
2.3 Simulations 4

3 A Mechanical Equivalent Of Chua's Circuit **9**
3.1 The Principle Behind Generating Negative Stiffness 10
3.2 Derivation Of A Linear Model 11
3.3 Constraints On The Mechanism 14
3.4 Equilibrium Points 15

4 Equivalence **18**
4.1 Nondimensional Governing Equations 18
4.2 Determining The Mechanical Parameters 19
4.3 Equivalence Constraints 20
4.4 The Region Of Equivalence 21

5 Conclusion **22**

A The Derivation Of The Reaction Force F_E **23**

B The Relation Between Negative Resistance And Mechanical Stiffness **26**

Bibliography **28**

1 Introduction

In this report a mechanical equivalent of the electrical Chua's circuit as proposed in [1] is analysed. The idea behind this mechanical Chua is that through the generation of a negative stiffness, a mechanical equivalent of the negative resistance in the electrical Chua is formed. The wide variety of dynamical behaviour that the relatively simple electrical Chua's circuit can generate makes the electrical Chua an interesting system. This wide variety of behaviour includes various types of bifurcations, period doubling and chaos.
The main issue in this report is to investigate if the proposed mechanical Chua is able to produce the same diverse dynamical behaviour as the electrical Chua. To do this the following two questions have to be answered. Is the proposed mechanical Chua able to produce a negative stiffness? How does the ability or inability of the proposed mechanical Chua to produce a negative stiffness influence its dynamical behaviour?
This report is organised as follows. First the electrical Chua is analysed. The governing equations of the electrical Chua are derived and the equilibrium points are calculated. The stability of the equilibrium points is examined and some simulations are performed to illustrate the diverse dynamic behaviour of the electrical Chua. After the analysis of the electrical Chua the mechanical Chua as proposed in [1] is analysed. The governing equations are derived and constraints acting on these governing equations are formulated. The equilibrium points of the mechanical Chua are calculated and their stability is analysed. Finally the equivalence of the electrical and mechanical Chua is analysed. The nondimensional governing equations of the electrical and mechanical Chua are formulated and compared to determine the parameters of the mechanical Chua. Equivalence constraints are formulated and the region of equivalence is investigated.

2 Chua's Circuit

Chua's circuit (see figure 2.1) is one of the simplest electrical systems that produces a wide variety of chaotic behaviour. It consists of four standard linear circuit components (2 capacitors, a resistor and a coil) and one nonlinear component (the piecewise linear resistor N_R). In this chapter the governing equations of Chua's circuit are presented. The equilibrium points of Chua's circuit are calculated and the influence of the linear resistance R on the equilibrium points is analysed. To illustrate the typical behaviour of Chua's circuit simulations of the governing equations are presented.

2.1 Governing Equations

The governing equations of Chua's circuit are of the following form:

$$C_1 \frac{dv_1}{dt} = \frac{1}{R}(v_2 - v_1) - f(v_1) \tag{2.1}$$

$$C_2 \frac{dv_2}{dt} = \frac{1}{R}(v_1 - v_2) + i_L \tag{2.2}$$

$$L \frac{di_L}{dt} = -v_2 \tag{2.3}$$

In these equations v_1 and v_2 represent the voltage difference over the capacitors C_1 and C_2 respectively. i_L is the current through the coil L. The piecewise linear function $f(v_1)$ represents the $v_R - i_R$ characteristic (see figure 2.2) of the nonlinear resistor N_R and is defined as follows.

$$f(v_1) = \begin{cases} G_b v_1 + (G_a - G_b)E & v_1 \geq E \\ G_a v_1 & |v_1| < E \\ G_b v_1 + (G_b - G_a)E & v_1 \leq -E \end{cases} \tag{2.4}$$

In this equation G_a and G_b are the slopes of the curves that characterise the nonlinear resistor R as shown in figure 2.2. The parameters G_a and G_b are negative and real. For the nonlinear resistor considered here the folowing relation between the parameters G_a and G_b also holds: $|G_b| < |G_a|$.
Because of the piecewise linear character of the nonlinear resistor N_R the state space of Chua's circuit can be divided into three separate regions for which a distinct linear set of governing equations holds. These regions are defined as $v_1 \geq E$, $-E < v_1 < E$ and $v_1 \leq -E$.

2.2 Equilibrium Points

The equilibrium points of Chua's circuit are calculated by requiring that the state variables $\mathbf{x} = (v_1 \quad v_2 \quad i_L)^T$ are constant with respect to time. This leads to the

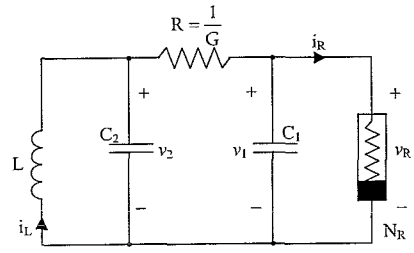

Figure 2.1: The circuit diagram of Chua's circuit with the nonlinear resistor N_R.

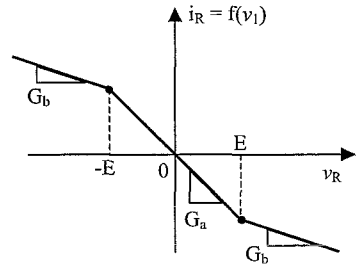

Figure 2.2: The piecewise linear v_R-i_R characteristic of the nonlinear resistor N_R.

following three equilibrium points.

$$\widetilde{\mathbf{x}}_e^+ = \left(\tfrac{G_b-G_a}{G_b+G}E \quad 0 \quad \tfrac{G_a-G_b}{G_b+G}EG\right) \tag{2.5}$$

$$\widetilde{\mathbf{x}}_e^0 = \begin{pmatrix}0 & 0 & 0\end{pmatrix} \tag{2.6}$$

$$\widetilde{\mathbf{x}}_e^- = \left(\tfrac{G_a-G_b}{G_b+G}E \quad 0 \quad \tfrac{G_b-G_a}{G_b+G}EG\right) \tag{2.7}$$

Where the conductance G defined as $G = 1/R$ is real and positive. Because of the piecewise linear character of the governing equations of Chua's circuit the equilibrium points $\widetilde{\mathbf{x}}_e^+$, $\widetilde{\mathbf{x}}_e^0$ and $\widetilde{\mathbf{x}}_e^-$ only exist if they lie in the appropriate regions of state space. The equilibrium point $\widetilde{\mathbf{x}}_e^0$ only exists if it lies in the region of state space defined by $-E < v_1 < E$. For the equilibrium point $\widetilde{\mathbf{x}}_e^0$ this is always true and therefore it always exists. The equilibrium points $\widetilde{\mathbf{x}}_e^+$ and $\widetilde{\mathbf{x}}_e^-$ only exist if they lie in the regions of state space defined by $v_1 \geq E$ and $v_1 \leq -E$ respectively. By combining these requirements with the equations (2.5) and (2.7) the following condition for the existence of the equilibrium points $\widetilde{\mathbf{x}}_e^+$ and $\widetilde{\mathbf{x}}_e^-$ can be defined.

$$\frac{G_b - G_a}{G_b + G}E \geq E \tag{2.8}$$

Making use of the signs of the parameters G_a and G_b and the relation $|G_b| < |G_a|$ equation (2.8) can be rewritten to the following relation between the parameters G, G_a and G_b.

$$-G_b < G < -G_a \tag{2.9}$$

This equation is equivalent to the following condition on the resistance R.

$$-\frac{1}{G_a} < R < -\frac{1}{G_b} \tag{2.10}$$

Stability Of The Equilibria

The stability of the equilibrium points of Chua's circuit is determined by calculating the eigenvalues of the linearisations around these equilibrium points. The linearisations around the equilibrium points $\widetilde{\mathbf{x}}_e^+$ and $\widetilde{\mathbf{x}}_e^-$ are identical. As a consequence these linearisations have identical eigenvalues and eigenvectors and therefore possess identical stability properties. The characteristic equations of the linearisations

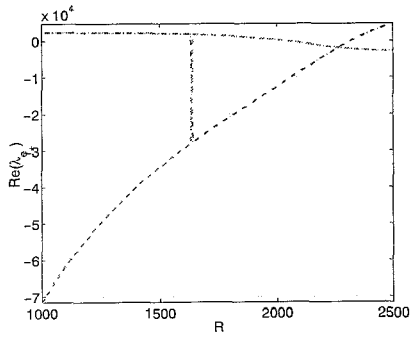

Figure 2.3: The real part of the eigenvalues of the linearisation of Chua's circuit around $\widetilde{\mathbf{x}}_e^+$ as a function of the resistance R.

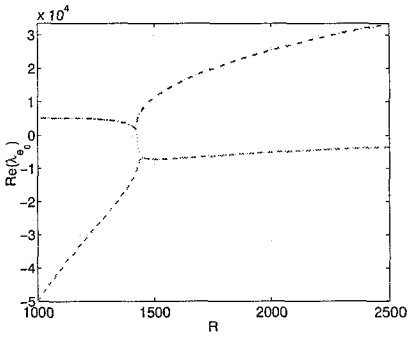

Figure 2.4: The real part of the eigenvalues of the linearisation of Chua's circuit around $\widetilde{\mathbf{x}}_e^0$ as a function of the resistance R.

around the equilibrium points $\widetilde{\mathbf{x}}_e^+$ and $\widetilde{\mathbf{x}}_e^0$ are of the following form.

$$\lambda_{e_+}^3 + \left(\frac{G}{C_2} + \frac{G_b + G}{C_1}\right)\lambda_{e_+}^2 + \left(\frac{1}{LC_2} + \frac{G_b G}{C_1 C_2}\right)\lambda_{e_+} + \frac{G_b + G}{C_1 C_2 L} = 0 \qquad (2.11)$$

$$\lambda_{e_0}^3 + \left(\frac{G}{C_2} + \frac{G_a + G}{C_1}\right)\lambda_{e_0}^2 + \left(\frac{1}{LC_2} + \frac{G_a G}{C_1 C_2}\right)\lambda_{e_0} + \frac{G_a + G}{C_1 C_2 L} = 0 \qquad (2.12)$$

Where λ_{e_+} and λ_{e_0} are the eigenvalues of the linearisations around $\widetilde{\mathbf{x}}_e^+$ and $\widetilde{\mathbf{x}}_e^0$ respectively. Equations (2.11) and (2.12) can be solved analytically but the resulting solutions are so complex that they are of little practical use. The real parts of the eigenvalues λ_{e_+} and λ_{e_0} are plotted as a function of the resistance R in the figures 2.3 and 2.4. The electrical parameters used in calculating these eigenvalues are defined in table 2.1.
Figure 2.3 shows the eigenvalues of the linearisation around the equilibrium point $\widetilde{\mathbf{x}}_e^+$ as a function of R. Because the equilibrium point $\widetilde{\mathbf{x}}_e^+$ only exists for values of R between $R = -1/G_a \approx 1423\,\Omega$ and $R = -1/G_b \approx 2315\,\Omega$ the eigenvalues shown in figure 2.3 are only valid for values of R between these values. Figure 2.3 shows that for values of R between approximately $R \approx 2048\,\Omega$ and $R = -1/G_b \approx 2315\,\Omega$ the equilibrium point $\widetilde{\mathbf{x}}_e^+$ is stable. This figure also shows that for $R \approx 1638.5\,\Omega$ two eigenvalues change sign.
Figure 2.4 shows that the equilibrium point $\widetilde{\mathbf{x}}_e^0$ is unstable for all values of R. One of the eigenvalues of the linearisation around $\widetilde{\mathbf{x}}_e^0$ is always positive, one eigenvalue is always negative and the remaining eigenvalue switches sign at $R = -1/G_a \approx 1423\Omega$.

2.3 Simulations

In order to illustrate the diverse dynamical behaviour of Chua's circuit simulations of the dimensional governing equations are carried out. In these simulations the electrical parameters as defined in table 2.1 are used. The resistance R is used as a bifurcation parameter and is therefore variable. Figures 2.5 through 2.18 show the behaviour of Chua's circuit for different values of R.
For $R = 2100\,\Omega$ the equilibria $\widetilde{\mathbf{x}}_e^+$ and $\widetilde{\mathbf{x}}_e^-$ are stable but the equilibrium point $\widetilde{\mathbf{x}}_e^0$ at the origin is unstable. In figures 2.5 and 2.6 simulation data of the stable equilibrium point $\widetilde{\mathbf{x}}_e^+$ is shown.
If R is decreased to $R = 2047.5\,\Omega$ the stable equilibria $\widetilde{\mathbf{x}}_e^+$ and $\widetilde{\mathbf{x}}_e^-$ become unstable and stable period 1 periodic orbits form around these equilibria. To determine

Parameter	Value
C_1	$10\,nF$
C_2	$100\,nF$
L	$22.0\,mH$
G_a	$-0.703\,mS$
G_b	$-0.432\,mS$
E	$2.002\,V$

Table 2.1: The parameters used in the simulations of the electrical Chua.

the period time and the Floquet multipliers of these periodic orbits the shooting method is used. For the periodic orbit around $\widetilde{\mathbf{x}}_e^+$ this leads to a period time of $T = 4.026 \cdot 10^{-4}\,[s]$ and to the Floquet multipliers $\gamma_1 = 0.014446$ and $\gamma_{2,3} = 1.00 \pm 1.984 \cdot 10^{-4} i$. Because Chua's circuit is an autonomous system at least one of the Floquet multipliers should be equal to one. The Floquet multipliers found with the shooting method do not fulfill this requirement because of numerical errors in their computation. A periodic orbit of an autonomous system is stable if all Floquet multipliers fulfill the following condition: $|\gamma| \leq 1$. For the Floquet multipliers found with the shooting method this requirement is not strictly satisfied because of numerical computation errors. Nevertheless the periodic orbits around $\widetilde{\mathbf{x}}_e^+$ and $\widetilde{\mathbf{x}}_e^-$ are stable. Simulation data of the periodic orbit around $\widetilde{\mathbf{x}}_e^+$ is shown in figures 2.7 and 2.8.

By decreasing R further to $R = 2020\,\Omega$ both stable period 1 periodic orbits become period 2 stable periodic orbits. The periodic orbit around the unstable equilibrium point $\widetilde{\mathbf{x}}_e^+$ has a period time of $T = 8.141 \cdot 10^{-4}\,[s]$ and the following Floquet multipliers: $\gamma_1 = -1.0471$, $\gamma_2 = -2.2905 \cdot 10^{-2}$ and $\gamma_3 = 1.0249$. Again because of numerical errors the Floquet multipliers do not strictly fulfill the stability condition while the periodic orbit is stable. Figures 2.9 and 2.10 show simulation data of the stable periodic orbit around $\widetilde{\mathbf{x}}_e^+$.

At $R = 1950\,\Omega$ the two stable periodic orbits around $\widetilde{\mathbf{x}}_e^+$ and $\widetilde{\mathbf{x}}_e^-$ have merged into one large periodic orbit. The period time of this periodic orbit is equal to $T = 4.256 \cdot 10^{-4}[s]$ and its Floquet multipliers are equal to $\gamma_1 = 5.0145 \cdot 10^{-3}$, $\gamma_2 = 1.4551$ and $\gamma_3 = 0.99999$. The Floquet multiplier γ_2 is real and larger than 1 and therefore the periodic orbit is unstable. Figures 2.11 and 2.12 show simulation data of the merged periodic orbit. If the initial state variables $\mathbf{x}_{\mathbf{e_0}}$ are chosen relatively close to the unstable periodic orbit the chaotic double scroll Chua attractor as shown in figures 2.13 and 2.14 is formed. For initial state variables $\mathbf{x}_{\mathbf{e_0}}$ relatively far from the unstable periodic orbit the behaviour of Chua's circuit is unstable i.e. solutions diverge.

By further decreasing the resistance R the trajectories tend to stay near the unstable periodic orbit longer before falling back to the double scroll attractor (see figures 2.15 and 2.16). For values of R below $R \approx 1785.82\,\Omega$ all possible trajectories are unbounded (see figures 2.17 and 2.18). This is due to a boundary crisis (i.e. the chaotic double scroll Chua attractor collides with the unstable periodic orbit) that occurs at approximately $R \approx 1785.82\,\Omega$ [2].

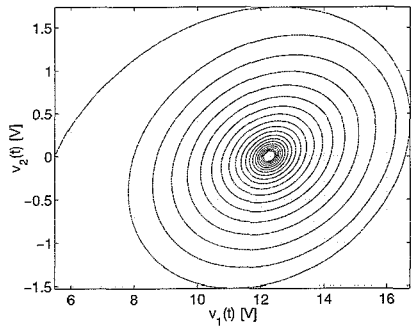

Figure 2.5: The phase plot of a simulation of Chua's circuit for $R = 2100\ \Omega$ and $\mathbf{x_{e_0}} = (5, 0, 0)$.

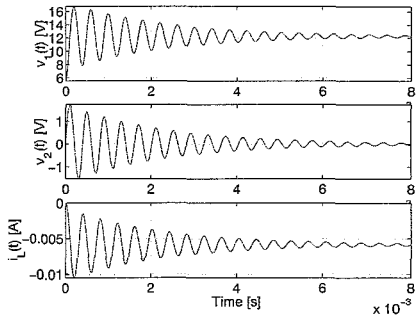

Figure 2.6: The different signals in the simulation of Chua's circuit for $R = 2100\ \Omega$ and $\mathbf{x_{e_0}} = (5, 0, 0)$.

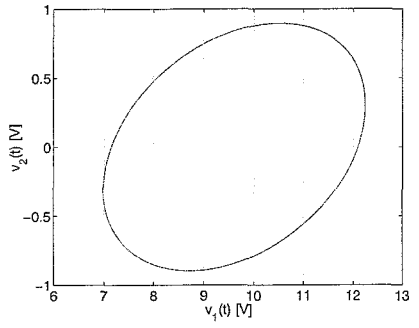

Figure 2.7: The phase plot of a simulation of Chua's circuit for $R = 2047.5\ \Omega$ and $\mathbf{x_{e_0}} = (11.9462, 0.6638, -0.0064)$.

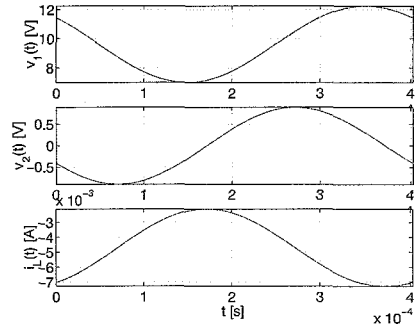

Figure 2.8: The different signals in the simulation of Chua's circuit for $R = 2047.5\ \Omega$ and $\mathbf{x_{e_0}} = (11.9462, 0.6638, -0.0064)$.

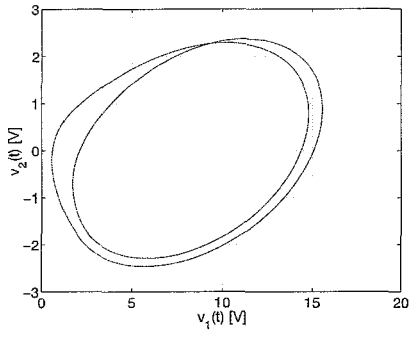

Figure 2.9: The phase plot of a simulation of Chua's circuit for $R = 2020\ \Omega$ and $\mathbf{x_{e_0}} = (12.7004, -1.2805, -0.0102)$.

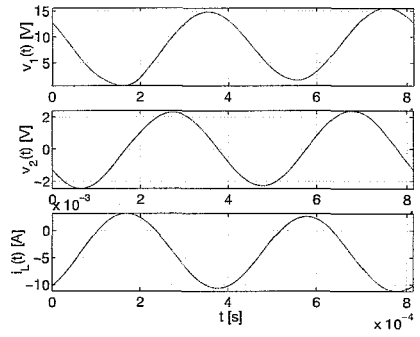

Figure 2.10: The different signals in the simulation of Chua's circuit for $R = 2020\ \Omega$ and $\mathbf{x_{e_0}} = (12.7004, -1.2805, -0.0102)$.

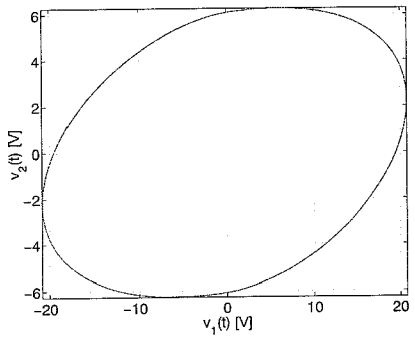

Figure 2.11: The phase plot of a simulation of Chua's circuit for $R = 1950\ \Omega$ and $\mathbf{x}_{e_0} = (10.9650, -4.1129, -0.0150)$.

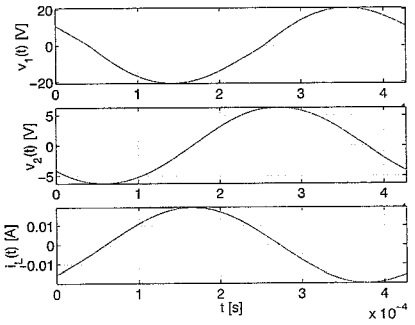

Figure 2.12: The different signals in the simulation of Chua's circuit for $R = 1950\ \Omega$ and $\mathbf{x}_{e_0} = (10.9650, -4.1129, -0.0150)$.

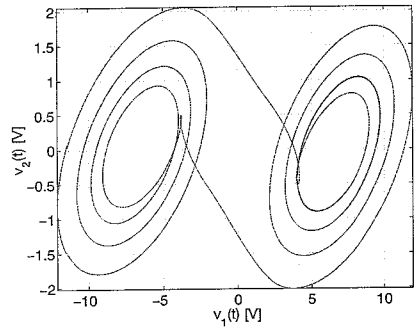

Figure 2.13: The phase plot of a simulation of Chua's circuit for $R = 1950\ \Omega$ and $\mathbf{x}_{e_0} = (8.9867, 0.4937, -0.0054)$.

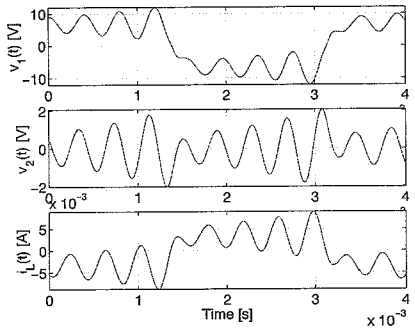

Figure 2.14: The different signals in the simulation of Chua's circuit for $R = 1950\ \Omega$ and $\mathbf{x}_{e_0} = (8.9867, 0.4937, -0.0054)$.

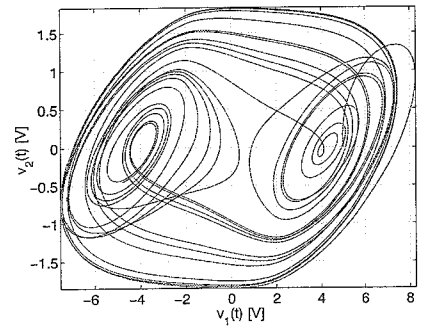

Figure 2.15: The phase plot of a simulation of Chua's circuit for $R = 1786\ \Omega$ and $\mathbf{x}_0 = (5, 0, 0)$.

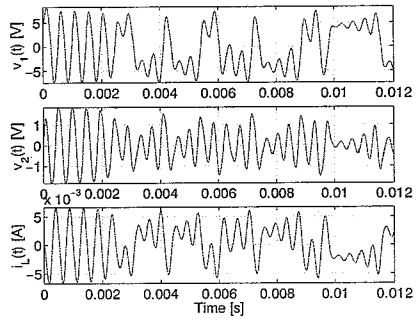

Figure 2.16: The different signals in the simulation of Chua's circuit for $R = 1786\ \Omega$ and $\mathbf{x}_0 = (5, 0, 0)$.

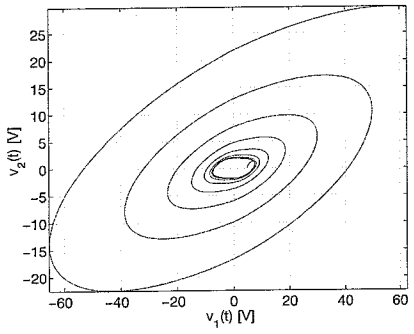

Figure 2.17: The phase plot of a simulation of Chua's circuit for $R = 1785\ \Omega$ and $\mathbf{x_0} = (5, 0, 0)$.

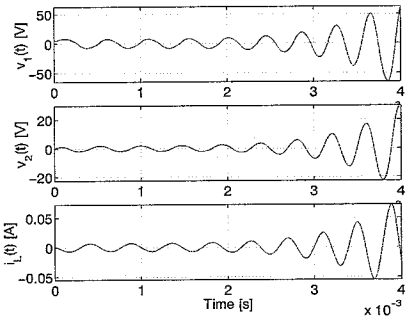

Figure 2.18: The different signals in the simulation of Chua's circuit for $R = 1785\ \Omega$ and $\mathbf{x_0} = (5, 0, 0)$.

3 A Mechanical Equivalent Of Chua's Circuit

In [1] mechanical equivalents of Chua's circuit are presented. In this chapter one of these mechanical equivalents will be analysed. First the principle behind generating a negative stiffness is explained. Then a linear model of the mechanical Chua is derived and the constraints that apply to the mechanical Chua are formulated. The equilibrium points of the mechanical Chua are calculated and compared to the equilibrium points of the electrical Chua.
The mechanical equivalent of Chua's circuit under consideration is shown in figure 3.1. The mechanical Chua shown in figure 3.1 can be divided in three separate mechanisms with one degree of freedom each. These mechanisms are coupled together through electromechanical devices.
The main part of the first mechanism (mechanism 1) is a rotating disc of radius r whose center is fixed in space and whose moment of inertia is negligible. Attached to this disc are a damper with damping coefficient c_1 and a spring with stiffness k_1. All springs and dampers used in the mechanical Chua are assumed to be linear

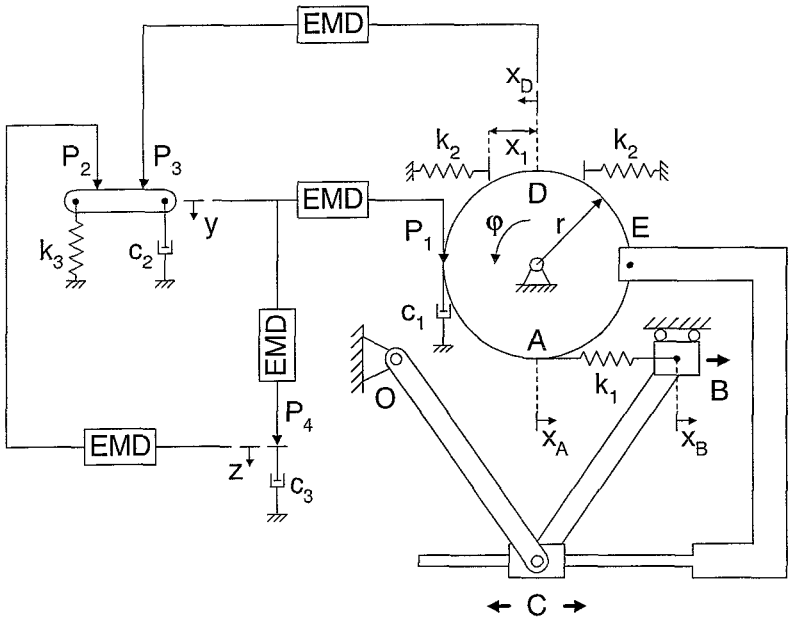

Figure 3.1: The first mechanical equivalent of Chua's circuit as presented in [1]. It consists of three separate mechanisms that are coupled together through electromechanical devices (EMD).

and massless. The spring with stiffness k_1 is also attached to the mechanism OCB which in turn is coupled to the rotating disc by the rigid rectangular frame CE. The connection between the rigid frame CE and the mechanism OCB is realised by a horizontal slider at point C. The point B of the mechanism OCB can only move in the horizontal direction and for small rotations of the disc is assumed to lie on a straight line together with the points O and A. For small rotations of the disc rotations of the rigid frame CE are assumed to be negligible. In effect this means that the vertical displacements of the points C and E are equal. In order for the mechanism to produce a piecewise-linear stiffness there are two springs with stiffness k_2 positioned on either side of point D at the top of the disc. These springs are only activated when the point D contacts one of the springs. All the forces acting on the mechanism are assumed to lie in the same plane as the center of gravity of the disc. In practise this can be achieved by a symmetric construction of the mechanism.
The second mechanism (mechanism 2) consists out of a damper with damping coefficient c_2 and a spring with stiffness k_3. This spring and damper are considered to be massless and connected to each other through a massless body. The third mechanism (mechanism 3) is a single massless damper with damping coefficient c_3. The three mechanisms are coupled to each other through electromechanical devices that exert the electromechanical forces P_1, P_2, P_3 and P_4 on the different mechanisms. Mechanism 1 is coupled to mechanism 2 through the electromechanical force P_1. Mechanism 2 is coupled to the mechanisms 1 and 3 through the electromechanical forces P_2 and P_3 respectively. Mechanism 3 is coupled to mechanism 1 through the electromechanical force P_4. The electromechanical forces P_1, P_2, P_3 and P_4 are proportional to the displacements of the different mechanisms as indicated in figure 3.1. The displacements x_A, x_B, x_D, y and z are positive in the directions indicated in figure 3.1.
There is an essential difference between the electrical and mechanical Chua. In the electrical Chua an implicit energy source is present in the form of the nonlinear resistor N_R. In the mechanical Chua (as presented here) there is no energy source. As a consequence it is very unlikely that the mechanical Chua can reproduce the diverse dynamical behaviour of Chua's circuit.

3.1 The Principle Behind Generating Negative Stiffness

The main idea behind the mechanical Chua shown in figure 3.1 is that the piecewise-linear negative resistance in Chua's circuit can be thought of as the electrical equivalent of a piecewise-linear negative stiffness. This equivalence between the electrical and mechanical system is based on the nondimensional governing equations of both systems. When the governing equations of the electrical and mechanical system are transformed to a nondimensional form the negative resistance and the negative stiffness produce identical terms (see appendix B).
In the mechanical Chua shown in figure 3.1 mechanism 1 is the mechanical equivalent of the electrical governing equation (2.1) and should therefore generate a negative stiffness. This negative stiffness is generated as follows. A counterclockwise rotation of the disc causes the point E and therefore the rigid frame CE connected to this point to move upwards. As a consequence the point B of the mechanism OCB moves to the right. If the mechanism OCB is constructed in such a way that the point B moves further to the right than the point A on the rotating disc then the spring with stiffness k_1 is stretched. This stretching of the spring causes it to exert a force on the disc in the direction of motion of point A. In effect this means that a small counterclockwise rotation of the disc creates a force on the disc at point

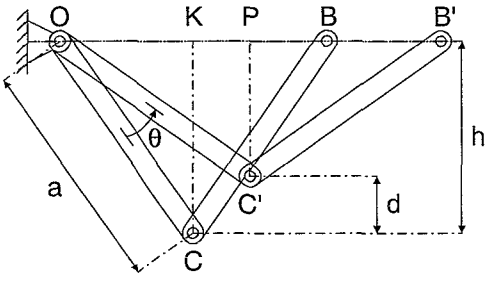

Figure 3.2: The mechanism OCB in its initial configuration (OCB) and after a counterclockwise rotation of the disc over an angle φ (OC'B').

A that tends to continue rotating the disc in the counterclockwise direction. This type of response is called a negative stiffness.
The mechanism OCB is also connected to the rotating disc at point E through the rigid frame CE. Because of this coupling the spring force at point A generates a reaction force at point E on the disc. This reaction force at point E works in the opposite direction of the spring force at point A, therefore mechanism 1 can only produce a negative stiffness if the reaction force at point E is smaller than the spring force at point A.

3.2 Derivation Of A Linear Model

In this section a linear model of the mechanical Chua shown in figure 3.1 is derived. The three mechanisms that make up the mechanical Chua are modeled separately. The total model of the mechanical Chua is obtained by joining the three separate models of the individual mechanisms.

Mechanism 1

The first mechanism considered is the rotating disc that is connected to the mechanism OCB. Because of the relatively large number of forces acting on the rotating disc the forces are determined separately. After the forces have been determined the equations governing the dynamics of the rotating disc are determined by requiring an equilibrium of moments that are acting on the disc.
The force that the spring with stiffness k_1 exerts on the rotating disc depends on the horizontal displacements of the points A and B. For small rotations φ around $\varphi = 0$ the horizontal displacement of point A can be written in the following form.

$$x_A = r \sin\varphi \approx r\varphi \tag{3.1}$$

The horizontal displacement of point B can be derived from the kinematics of the mechanism OCB and the rigid frame CE. A schematic drawing of the mechanism OCB is shown in figure 3.2. For a counterclockwise rotation of the disc over an angle φ the point B moves from its initial position B at $\varphi = 0$ to the position B'. The horizontal displacement of the point B can be expressed as:

$$\begin{aligned} x_B \equiv BB' &= 2\,(OP - OK) \\ &= 2\left(\sqrt{a^2 - (h-d)^2} - \sqrt{a^2 - h^2}\right) \end{aligned} \tag{3.2}$$

The rigid frame CE couples the vertical displacement of the point E on the disc to the vertical displacement of the point C in the mechanism OCB. For small rotations φ of the disc rotations of the frame CE are negligible. The vertical displacement of the point C can be written as:

$$d = r \sin \varphi \tag{3.3}$$

Substituting this relation into equation (3.2) leads to the following expression for the horizontal displacement of the point B:

$$x_B = 2\left(\sqrt{a^2 - (h - r\sin\varphi)^2} - \sqrt{a^2 - h^2}\right) \tag{3.4}$$

The above expression for x_B is clearly not equal to the expression found in [1]. The expression found in [1] is obtained by applying a first order approximation to equation (3.4) around $\varphi = 0$. This leads to the following expression for the horizontal displacement of the point B.

$$\begin{aligned} x_B(\varphi) &\approx x_B(\varphi = 0) + \frac{dx_B}{d\varphi}(\varphi = 0) \cdot \varphi \\ &= \frac{2hr}{\sqrt{a^2 - h^2}}\varphi \end{aligned} \tag{3.5}$$

Using equations (3.1) and (3.5) and assuming that for small rotations φ the points O, A and B lie approximately on a straight line the spring force F_A can be written as:

$$\begin{aligned} F_A &= k_1 (x_B - x_A) \\ &= k_1 \left(\frac{2h}{\sqrt{a^2 - h^2}} - 1\right) r\varphi \end{aligned} \tag{3.6}$$

Because of the coupling between the rotating disc and the mechanism OCB through the rigid frame CE a reaction force F_E is exerted on the disc at point E. This reaction force results from the spring force F_A that acts on the mechanism OCB at point B. For this reaction force the following relation holds (see appendix A):

$$F_E = 2k_1 \left(\frac{2h}{\sqrt{a^2 - h^2}} - 1\right)\left(\frac{h}{\sqrt{a^2 - h^2}}\right) r\varphi \tag{3.7}$$

The springs with stiffness k_2 are only "active" when the horizontal displacement of point D is larger respectively smaller than the gap x_1. In other words the springs with stiffness k_2 only exert a force on the rotating disc if $x_D > x_1$ or $x_D < -x_1$ respectively. For small rotations φ the contact angle φ^* can be defined as $\varphi^* = \frac{x_1}{r}$. The spring force F_D can now written as:

$$F_D = \begin{cases} -k_2 r(\varphi - \varphi^*) & \varphi \geq \varphi^* \\ 0 & |\varphi| < \varphi^* \\ -k_2 r(\varphi + \varphi^*) & \varphi \leq -\varphi^* \end{cases} \tag{3.8}$$

The forces generated by the electromechanical actuator and the damper at point F can for small rotations φ be written as:

$$P_1 = \lambda_1 y \tag{3.9}$$

$$F_{c_1} = c_1 r\dot{\varphi}\cos\varphi \approx c_1 r\dot{\varphi} \tag{3.10}$$

Where λ_1 is a constant of proportionality that relates the vertical displacement of mechanism 2 to the electromechanical force P_1.

Based on the free body diagram of the rotating disc shown in figure 3.3 the equation of motion of the disc can be written as:

$$I\ddot{\varphi} = F_A r - F_E r + P_1 r + F_D r - F_{c_1} r \tag{3.11}$$

The terms $F_A r$ and $-F_E r$ in the equation of motion (3.11) can be combined into one term by making use of the expressions for F_A and F_E as defined by equations (3.6) and (3.7) respectively.

$$F_A r - F_E r = k_1 \left(\frac{2h}{\sqrt{a^2 - h^2}} - 1 \right) \left(1 - \frac{2h}{\sqrt{a^2 - h^2}} \right) r^2 \varphi \tag{3.12}$$

$$= k_1 \delta r^2 \varphi \tag{3.13}$$

The geometrical constant δ is defined as:

$$\delta = \left(\frac{2h}{\sqrt{a^2 - h^2}} - 1 \right) \left(1 - \frac{2h}{\sqrt{a^2 - h^2}} \right) \tag{3.14}$$

$$= - \left(\frac{2h}{\sqrt{a^2 - h^2}} - 1 \right)^2 \tag{3.15}$$

Combining the definition of the geometrical constant δ with equation (3.13) shows that by definition the spring force F_A is always smaller than the reaction force F_E. Substituting the relations describing the different forces into equation (3.11) and combining the terms $F_A r$ and $-F_E r$ leads to the following second order equation of motion:

$$I\ddot{\varphi} = \begin{cases} -c_1 r^2 \dot{\varphi} + k_1 \delta r^2 \varphi - k_2 r^2 (\varphi - \varphi^*) + \lambda_1 r y & \varphi \geq \varphi^* \\ -c_1 r^2 \dot{\varphi} + k_1 \delta r^2 \varphi + \lambda_1 r y & |\varphi| < \varphi^* \\ -c_1 r^2 \dot{\varphi} + k_1 \delta r^2 \varphi - k_2 r^2 (\varphi + \varphi^*) + \lambda_1 r y & \varphi \leq -\varphi^* \end{cases} \tag{3.16}$$

The equation of motion (3.16) can be rewritten as a first order differential equation by neglecting the moment of inertia of the disc. This leads to the following first order equation of motion.

$$\dot{\varphi} = \begin{cases} \frac{k_1 \delta}{c_1} \varphi - \frac{k_2}{c_1} (\varphi - \varphi^*) + \frac{\lambda_1}{c_1 r} y & \varphi \geq \varphi^* \\ \frac{k_1 \delta}{c_1} \varphi + \frac{\lambda_1}{c_1 r} y & \varphi < \varphi^* \\ \frac{k_1 \delta}{c_1} \varphi - \frac{k_2}{c_1} (\varphi + \varphi^*) + \frac{\lambda_1}{c_1 r} y & \varphi \leq -\varphi^* \end{cases} \tag{3.17}$$

At a first glance this first order equation of motion seems to be similar to the equation of motion found in [1] but this is not the case. The definition of the geometrical constant δ differs from the definition of δ used in [1] and consequently the equation of motion (3.17) is not identical to the equation of motion found in [1].

Mechanism 2

The free body diagram of the second mechanism that is part of the mechanical Chua is shown in figure 3.4. For the electromechanical forces acting on the second mechanism the following equations hold:

$$P_2 = \lambda_2 z \qquad\qquad P_3 = \lambda_3 r \varphi \tag{3.18}$$

The constants λ_2 and λ_3 are constants of proportionality that relate the displacements z and x_D to the electromechanical forces P_2 and P_3 respectively. For the

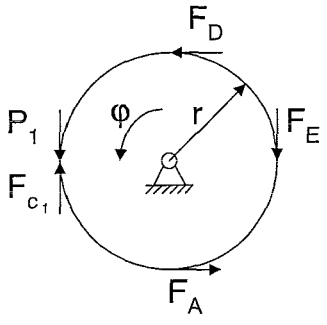

Figure 3.3: The free body diagram of the rotating disc that is part of mechanism 1.

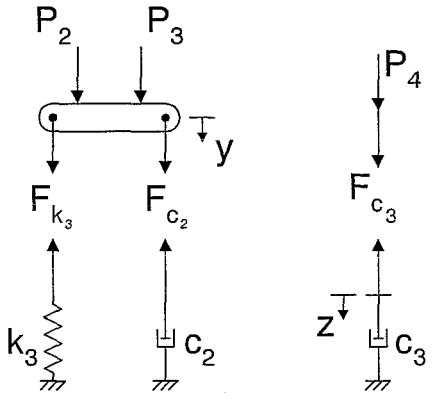

Figure 3.4: The free body diagrams of mechanism 2 (left) and mechanism 3 (right).

forces produced by the spring with stiffness k_3 and the damper with damping coefficient c_2 the following relations hold.

$$F_{c_2} = -c_2\dot{y} \qquad\qquad F_{k_3} = -k_3 y \tag{3.19}$$

Neglecting the mass of the object that connects the spring to the damper the equation of motion of mechanism 2 can be written as:

$$\dot{y} = \frac{\lambda_3 r}{c_2}\varphi - \frac{k_3}{c_2}y + \frac{\lambda_2}{c_2}z \tag{3.20}$$

Mechanism 3

Mechanism 3 consists of a single massless damper with damping coefficient c_3. The free body diagram of this damper is shown in figure 3.4. The forces acting on the damper can be described by the following equations.

$$F_{c_3} = -c_3\dot{z} \qquad\qquad P_4 = -\lambda_4 y \tag{3.21}$$

The constant of proportionality λ_4 relates the vertical displacement y to the electromechanical force P_4. Using the above expressions for the forces acting on the damper the equation of motion of mechanism 2 can be written in the following form.

$$\dot{z} = -\frac{\lambda_4}{c_3}y \tag{3.22}$$

3.3 Constraints On The Mechanism

There are two types of constraints that apply to the mechanical Chua. The first type of constraint is based on the physical limitations of the mechanism. The second type of constraint results from the requirement that mechanism 1 has to produce a negative stiffness.

Physical Constraints

The physical constraints that apply to the mechanical Chua limit the ways in which the model parameters can be chosen because of physical limits. There are two

physical constraints that apply to the mechanical equivalent of Chua's circuit. The first and most general of these constraints is the requirement that all mechanical parameters are real.

$$k_1, k_2, k_3, c_1, c_2, c_3, r, a, h, x_1 \in \mathbb{R}^+ \tag{3.23}$$

$$\lambda_1, \lambda_2, \lambda_3, \lambda_4, \delta \in \mathbb{R} \tag{3.24}$$

The second constraint is based on geometric limitations and can be expressed as:

$$h \leq a \tag{3.25}$$

Constraint equation (3.25) limits the parameter h as a function of the parameter a. This constraint results from the fact that it is physically impossible to choose the parameter h larger than the parameter a. This can be understood by examining figure 3.2 in which the parameters h and a are defined.

Negative Stiffness Constraints

To guarantee that mechanism 1 produces a negative stiffness two constraints have to be placed on this mechanism. The first of these constraints is needed to ensure that the spring with stiffness k_1 is stretched for a rotation φ in the counterclockwise direction, thereby generating a negative stiffness. The second constraint is needed to ensure that the reaction force F_E is smaller than the spring force F_A which guarantees that the "net spring force" is indeed a negative stiffness spring force. These two negative stiffness constraints can be formulated as follows.

$$|x_B| > |x_A| \tag{3.26}$$

$$|F_A| > |F_E| \tag{3.27}$$

By substituting the relations for x_A and x_B into constraint equation (3.26) and after dividing the rotation φ and the radius r out of equation (3.26) it can be rewritten in the following form.

$$h > \frac{1}{5}\sqrt{5}a \tag{3.28}$$

By making use of the definition of δ as defined by equation (3.15) constraint equation (3.27) can be replaced by the following constraint on the geometrical constant δ.

$$\delta > 0 \tag{3.29}$$

This constraint equation cannot be satisfied because the geometrical constant δ is by definition always negative. As a consequence mechanism 1 cannot produce a negative stiffness. Consequently the mechanical Chua is unable to produce the same diverse dynamical behaviour as Chua's circuit.

3.4 Equilibrium Points

The equilibrium points of the mechanical Chua are determined by requiring that the governing equations (3.17), (3.20) and (3.22) are constant with respect to time (i.e. $\frac{d\varphi}{dt} = \frac{dy}{dt} = \frac{dz}{dt} = 0$). This leads to the following three equilibrium points.

$$\widetilde{\mathbf{x}}_m^+ = \begin{pmatrix} -\frac{k_2}{k_1\delta - k_2}\varphi^* & 0 & \frac{k_2 r}{k_1\delta - k_2}\frac{\lambda_3}{\lambda_2}\varphi^* \end{pmatrix} \tag{3.30}$$

$$\widetilde{\mathbf{x}}_m^0 = \begin{pmatrix} 0 & 0 & 0 \end{pmatrix} \tag{3.31}$$

$$\widetilde{\mathbf{x}}_m^- = \begin{pmatrix} \frac{k_2}{k_1\delta - k_2}\varphi^* & 0 & -\frac{k_2 r}{k_1\delta - k_2}\frac{\lambda_3}{\lambda_2}\varphi^* \end{pmatrix} \tag{3.32}$$

These equilibrium points only exists if they lie in the appropriate regions of state space. The equilibrium point $\widetilde{\mathbf{x}}_m^0$ always exists because it always lies in the region of state space defined by $-\varphi^* < \varphi < \varphi^*$. The equilibrium points $\widetilde{\mathbf{x}}_m^+$ and $\widetilde{\mathbf{x}}_m^-$ only exist if the following condition holds:

$$-\frac{k_2}{k_1\delta - k_2}\varphi^* > \varphi^* \tag{3.33}$$

Because the parameters k_1, k_2 and φ^* are constant, real and positive equation (3.33) can be transformed to the following restriction on δ.

$$\delta \in \left[0, \tfrac{k_2}{k_1}\right] \tag{3.34}$$

The geometrical constant δ is by definition always negative (see equation (3.15)). As a consequence the above restriction of δ is never satisfied and the equilibrium points $\widetilde{\mathbf{x}}_m^+$ and $\widetilde{\mathbf{x}}_m^-$ cannot exist. This result can also be interpreted in the following way. Because the geometrical constant δ is by definition always negative the mechanical Chua is unable to produce a negative stiffness. This limits the region of electrical parameter space where the mechanical Chua might be equivalent to the electrical Chua to the region where the electrical equilibria $\widetilde{\mathbf{x}}_e^+$ and $\widetilde{\mathbf{x}}_e^-$ do not exist (i.e. $R < -1/G_a$). This also corresponds to the region of the electrical parameter space where the electrical Chua cannot produce any chaotic dynamic behaviour. This means that even if the mechanical Chua is equivalent to the electrical Chua the mechanical Chua will not be able to produce chaotic dynamical behaviour.

Stability Of The Equilibria

The stability of the mechanical equilibria is determined by examining the eigenvalues of the linearisations around the respective equilibria. Because the mechanical parameters cannot be chosen in such a way that the equilibria $\widetilde{\mathbf{x}}_m^+$ and $\widetilde{\mathbf{x}}_m^-$ exist it does not make sense to calculate the eigenvalues of the linearisations around these equilibria. The only equilibrium point of interest is the equilibrium point $\widetilde{\mathbf{x}}_m^0$ at the origin. For this equilibrium point the following characteristic equation can be derived from the linearisation.

$$\lambda_{m_0}^3 + \left(\frac{k_3}{c_2} - \frac{k_1\delta}{c_1}\right)\lambda_{m_0}^2 + \left(\frac{\lambda_2\lambda_4}{c_2c_3} - \frac{\lambda_1\lambda_3 + k_1k_3\delta}{c_1c_2}\right)\lambda_{m_0} + \frac{k_1\delta\lambda_2\lambda_4}{c_1c_2c_3} = 0 \tag{3.35}$$

In this equation λ_{m_0} are the eigenvalues of the linearisation around the equilibrium point $\widetilde{\mathbf{x}}_m^0$. The eigenvalues calculated from equation (3.35) are only useful if they can be compared to the eigenvalues of the electrical Chua. To achieve this the equivalence conditions derived in chapter 4 are used. Based on the expressions of the mechanical parameters as defined by equations (4.15), (4.16) and (4.17) the eigenvalues of the mechanical Chua can be calculated as a function of the electrical resistance R. To ensure that the mechanical parameters are feasible the equivalence constraints (4.23) and (4.25) have to be satisfied. This means that the eigenvalues of the mechanical Chua that are calculated in this way are only meaningful for values of R satisfying $R < -1/G_a$. In figure 3.5 the real parts of the eigenvalues λ_{m_0} of the mechanical Chua are shown as a function of the resistance R. Comparing the eigenvalues of the electrical Chua shown in figure 2.4 to the eigenvalues of the mechanical Chua shown in figure 3.5 shows that the eigenvalues for both systems are identical. This means that for $R < -1/G_a$ the stability properties of the equilibrium point at the origin are identical for the electrical and mechanical systems.

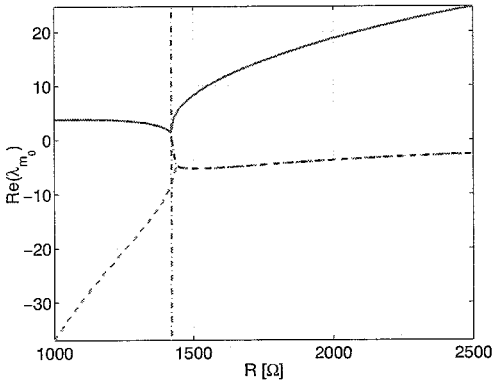

Figure 3.5: The real parts of the eigenvalues of the linearisation of the mechanical Chua around the equilibrium point $\widetilde{\mathbf{x}}_m^0$ as a function of the resistance R. The vertical line indicates the point where $R = -\frac{1}{G_a}$.

4 Equivalence

The equivalence between the electrical and mechanical Chua is based on the nondimensional governing equations of both systems. By requiring that the nondimensional governing equations of the mechanical Chua are identical to the nondimensional governing equations of the electrical Chua the parameters of the mechanical Chua can be determined. Based on these mechanical parameters the possibility of equivalence between the electrical and mechanical systems can be investigated. Comparing the mechanical parameter values required for equivalence with the feasible mechanical parameters values leads to limitations on the electrical parameters. Finally the region of equivalence is investigated and simulations are performed to show that both systems are equivalent.

4.1 Nondimensional Governing Equations

The nondimensional governing equations of the electrical and mechanical Chua are determined by scaling the dimensional state variables with the appropriate constants. This scaling of the dimensional state variables is straightforward for the electrical Chua. For the mechanical Chua the scaling constants are not chosen in advance but determined from the equations that arise when requiring equivalence between the electrical and mechanical Chua.

Chua's Circuit

To obtain the nondimensional governing equations of Chua's circuit the dimensional state variables v_1, v_2, i_L and t are scaled with the system parameters E, G and C_2. This leads to the following expressions for the nondimensional state variables x, y, z and τ.

$$x \equiv \frac{v_1}{E} \qquad y \equiv \frac{v_2}{E} \qquad z \equiv \frac{i_L}{EG} \qquad \tau \equiv \frac{G}{C_2}t \tag{4.1}$$

Substituting the equations describing the relations between the dimensional and nondimensional state variables in the dimensional governing equations (2.1), (2.2) and (2.3) leads to the following set of nondimensional electrical governing equations.

$$\frac{dx}{d\tau} = \begin{cases} -\frac{C_2}{C_1}\left(\frac{G_b+G}{G}\right)x + \frac{C_2}{C_1}y + \frac{C_2}{C_1}\left(\frac{G_b-G_a}{G}\right) & x \geq 1 \\ -\frac{C_2}{C_1}\left(\frac{G_a+G}{G}\right)x + \frac{C_2}{C_1}y & |x| < 1 \\ -\frac{C_2}{C_1}\left(\frac{G_b+G}{G}\right)x + \frac{C_2}{C_1}y + \frac{C_2}{C_1}\left(\frac{G_a-G_b}{G}\right) & x \leq -1 \end{cases} \tag{4.2}$$

$$\frac{dy}{d\tau} = x - y + z \tag{4.3}$$

$$\frac{dz}{d\tau} = -\frac{C_2}{LG^2}y \tag{4.4}$$

Mechanical Chua

The mechanical governing equations (3.17), (3.20) and (3.22) describing the mechanical Chua can be written in a nondimensional form by defining the nondimensional state variables $\widetilde{\varphi}$, $\widetilde{y}$, $\widetilde{z}$ and τ as follows.

$$\varphi = \varphi^* \widetilde{\varphi} \qquad y = y^* \widetilde{y} \qquad z = z^* \widetilde{z} \qquad \tau = \omega t \tag{4.5}$$

The parameters φ^*, y^*, z^* and ω are constants of proportionality that are used to scale between the dimensional and the nondimensional state variables. Substituting the nondimensional variables defined by the equations (4.5) into the governing equations (3.17), (3.20) and (3.22) leads to the following set of nondimensional mechanical governing equations.

$$\frac{d\widetilde{\varphi}}{d\tau} = \begin{cases} \left(\frac{k_1\delta - k_2}{c_1\omega}\right)\widetilde{\varphi} + \frac{\lambda_1 y^*}{c_1\omega r\varphi^*}\widetilde{y} + \frac{k_2}{c_1\omega} & \widetilde{\varphi} \geq 1 \\ \frac{k_1\delta}{c_1\omega}\widetilde{\varphi} + \frac{\lambda_1 y^*}{c_1\omega r\varphi^*}\widetilde{y} & |\widetilde{\varphi}| < 1 \\ \left(\frac{k_1\delta - k_2}{c_1\omega}\right)\widetilde{\varphi} + \frac{\lambda_1 y^*}{c_1\omega r\varphi^*}\widetilde{y} - \frac{k_2}{c_1\omega} & \widetilde{\varphi} \leq -1 \end{cases} \tag{4.6}$$

$$\frac{d\widetilde{y}}{d\tau} = \frac{\lambda_3 r\varphi^*}{c_2\omega y^*}\widetilde{\varphi} - \frac{k_3}{c_2\omega}\widetilde{y} + \frac{\lambda_2 z^*}{c_2\omega y^*}\widetilde{z} \tag{4.7}$$

$$\frac{d\widetilde{z}}{d\tau} = -\frac{\lambda_4 y^*}{c_3\omega z^*}\widetilde{y} \tag{4.8}$$

4.2 Determining The Mechanical Parameters

The parameters of the mechanical Chua are determined by requiring that the nondimensional governing equations of the mechanical Chua are identical to the nondimensional governing equations of the electrical Chua. This is achieved by requiring that the "parameters" in the mechanical nondimensional governing equations are identical to the "parameters" in the electrical nondimensional governing equations. Using the nondimensional governing equations for the electrical and mechanical Chua as defined by equations (4.2), (4.3), (4.4) and (4.6), (4.7), (4.8) respectively this leads to the following relations between the electrical and mechanical parameters.

$$\frac{k_1\delta}{c_1\omega} = -\frac{C_2}{C_1}\left(\frac{G_a + G}{G}\right) \qquad \frac{\lambda_3 r\varphi^*}{c_2\omega y^*} = 1 \tag{4.9}$$

$$\frac{k_2}{c_1\omega} = \frac{C_2}{C_1}\left(\frac{G_b - G_a}{G}\right) \qquad \frac{k_3}{c_2\omega} = 1 \tag{4.10}$$

$$\frac{\lambda_1 y^*}{c_1\omega r\varphi^*} = \frac{C_2}{C_1} \qquad \frac{\lambda_2 z^*}{c_2\omega y^*} = 1 \tag{4.11}$$

$$\frac{\lambda_4 y^*}{c_3\omega z^*} = \frac{C_2}{LG^2} \qquad \varphi^* = \frac{x_1}{r} \tag{4.12}$$

Because the number of mechanical parameters is larger than the number of equations a unique solution for the mechanical parameters cannot be obtained from the above set of equations. Effectively nine of the mechanical parameters can be chosen freely. The other eight mechanical parameters are determined by the electrical parameters and the nine freely chosen mechanical parameters. Here the free mechanical parameters are chosen so that the following expressions are obtained for the mechanical parameters φ^*, y^*, z^*, ω, λ_3, λ_4, δ and k_3.

$$\varphi^* = \frac{x_1}{r} \qquad z^* = \frac{k_2^2 x_1}{\lambda_1\lambda_2}\frac{c_2}{c_1}C_1C_2\left(\frac{G}{G_b - G_a}\right)^2 \tag{4.13}$$

$$y^* = \frac{k_2 x_1}{\lambda_1}\frac{G}{G_b - G_a} \qquad \omega = \frac{k_2}{c_1}\frac{C_1}{C_2}\frac{G}{G_b - G_a} \tag{4.14}$$

$$\lambda_3 = \frac{k_2^2}{\lambda_1}\frac{c_2}{c_1}\frac{C_1}{C_2}\left(\frac{G}{G_b - G_a}\right)^2 \tag{4.15}$$

$$\lambda_4 = \frac{k_2^2}{\lambda_2}\frac{c_2 c_3}{c_1^2}\frac{C_2}{LG^2}\left(\frac{C_1}{C_2}\right)^2\left(\frac{G}{G_b - G_a}\right)^2 \tag{4.16}$$

$$\delta = -\frac{k_2}{k_1}\frac{G_a + G}{G_b - G_a} \qquad k_3 = k_2\frac{c_2}{c_1}\frac{C_1}{C_2}\frac{G}{G_b - G_a} \tag{4.17}$$

If the parameters of the mechanical Chua are chosen as defined by the above equations then the nondimensional governing equations of the electrical and mechanical systems are identical. As a consequence the nondimensional state variables of both systems are identical. This leads to the following relations between the dimensional state variables of the electrical and mechanical system.

$$\varphi = \frac{\varphi^*}{E}v_1 \qquad y = \frac{y^*}{E}v_2 \tag{4.18}$$

$$z = \frac{z^*}{EG}i_L \qquad t_m = \frac{G}{c_2\omega}t_e \tag{4.19}$$

In the above equations the variables t_e and t_m are the time variables of the electrical and mechanical system respectively

4.3 Equivalence Constraints

The validity of the parametrisation of the mechanical Chua proposed in the previous section is limited by the feasible values of the mechanical parameters δ and k_3. The spring stiffness k_3 should always be real and positive and the geometrical constant δ is by definition always real and negative. These two constraints can be expressed as:

$$k_3 > 0 \tag{4.20}$$

$$\delta < 0 \tag{4.21}$$

Using the expression for k_3 as defined by equation (4.17) constraint equation (4.20) can written in the following form.

$$k_2\frac{c_2}{c_1}\frac{C_1}{C_2}\frac{G}{G_b - G_a} > 0 \tag{4.22}$$

All parameters in this constraint equation are real and positive with the exception of G_a and G_b which are real and negative. By making use of the signs of the parameters constraint equation (4.22) can reduced to the following expression.

$$|G_b| < |G_a| \tag{4.23}$$

The constraint on δ as defined by constraint equation (4.21) can be written in the following form by making use of the definition of δ given by equation (4.17).

$$-\frac{k_2}{k_1}\frac{G_a + G}{G_b - G_a} < 0 \tag{4.24}$$

Again the parameters in this equation are all real and positive with the exception of G_a and G_b which are real and negative. By using the signs of the parameters and by making use of constraint equation (4.23) constraint equation (4.24) can be reduced to the following expression.

$$G > |G_a| \tag{4.25}$$

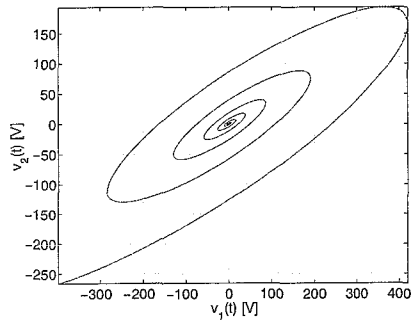

Figure 4.1: A simulation of the electrical Chua for $R = 1400\,\Omega$ and $\mathbf{x}_{e_0} = (1, 0, 0)$.

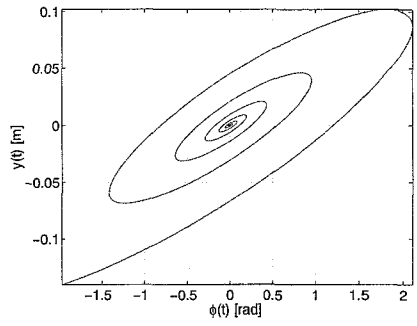

Figure 4.2: A simulation of the mechanical Chua for $R = 1400\ \Omega$ and $\mathbf{x}_{m_0} = (5.0 \cdot 10^{-3}, 0, 0)$.

This constraint equation is equivalent to the following constraint on the electrical resistance R.

$$R < -\frac{1}{G_a} \tag{4.26}$$

Constraint equations (4.23) and (4.26) are not mutually exclusive and therefore the mechanical parameters can be chosen in such a way that the dynamical behaviour of the electrical and mechanical Chua is identical in a qualitative sense.
Constraint equation (4.26) corresponds with the results obtained from the existence of the mechanical equilibria. The values of electrical resistance R allowed by constraint equation (4.26) correspond to the values of R for which the electrical equilibria $\widetilde{\mathbf{x}}_e^+$ and $\widetilde{\mathbf{x}}_e^-$ do not exist.

4.4 The Region Of Equivalence

Because the mechanical Chua is unable to produce a negative stiffness the electrical parameters for which the mechanical Chua is equivalent to the electrical Chua are limited by the constraint equations (4.23) and (4.26). If the electrical parameters are chosen as defined in table 2.1 this leads to the following restriction on the electrical resistance R.

$$R < -\frac{1}{G_a} \approx 1422\ \Omega \tag{4.27}$$

For these values of R the electrical Chua possesses only unbounded trajectories. There are no periodic solutions or chaotic behaviour. For the values of R defined by equation (4.27) the dynamical behaviour of the mechanical Chua is identical to the dynamical behaviour of the electrical Chua. Therefore the dynamical behaviour of the mechanical Chua does not have periodic solutions or chaotic behaviour.
The absence of periodic solutions and chaotic behaviour in the dynamics of the mechanical Chua is a direct consequence of the inability of the mechanical Chua to produce a negative stiffness. Constraint equation (4.26) exists because the geometrical constant δ is by definition smaller than zero i.e. the mechanical Chua is unable to produce a negative stiffness. Figures 4.1 and 4.2 show a simulation for the electrical and mechanical Chua starting from equivalent initial conditions. These figures clearly show that the dynamical behaviour of both systems is unstable.

5 Conclusion

The mechanical equivalent of Chua's circuit as defined in [1] is unable to generate a negative stiffness. The consequence of this inability is that the mechanical Chua cannot produce periodic solutions or chaotic behaviour. The mechanical Chua is equivalent to the electrical Chua but only for electrical parameters for which all possible trajectories of the electrical Chua are unbounded. This makes the equivalence between the electrical and mechanical Chua rather pointless. Because all mechanical equivalents of Chua's circuit proposed in [1] are based on the same principle of generating a negative stiffness none of these mechanical equivalents will be able to reproduce the diverse dynamical behaviour of Chua's circuit.

A The Derivation Of The Reaction Force F_E

The reaction force F_E originates from the mechanical coupling that is formed by the rigid rectangular frame CE between the point C of the mechanism OCB and the point E of the rotating disc. Through this mechanical coupling the spring force F_A acting on point A of the disc is transmitted back to the point E of the disc. This reaction force F_E can be determined by analysing the equilibrium of forces and moments of the mechanism OCB as described in [3]. A free body diagram of mechanism 1 is shown in the figures A.1 and A.2. From these figures the following nine equilibrium conditions for the mechanism OCB and the rigid frame CE can be derived:

$$-F_B^x - F_A = 0 \tag{A.1}$$

$$-F_B^y - F_N = 0 \tag{A.2}$$

$$F_B^y - F_C^y - \frac{1}{2}F_W = 0 \tag{A.3}$$

$$F_B^x - F_C^x = 0 \tag{A.4}$$

$$\begin{aligned}\frac{1}{2}a\left(-F_B^x \sin\theta_1 + F_B^y \cos\theta_1\right) + \frac{1}{2}a\left(-F_C^x \sin\theta_1 + F_C^y \cos\theta_1\right) \\ + \frac{1}{4}aF_W \cos\theta_1 = 0\end{aligned} \tag{A.5}$$

$$F_C^x - F_O^x = 0 \tag{A.6}$$

$$F_O^y + F_C^y - \frac{1}{2}F_W = 0 \tag{A.7}$$

$$\begin{aligned}\frac{1}{2}a\left(F_O^x \sin\theta_1 - F_O^y \cos\theta_1\right) + \frac{1}{2}a\left(F_C^x \sin\theta_1 + F_C^y \cos\theta_1\right) \\ - \frac{1}{4}aF_W \cos\theta_1 = 0\end{aligned} \tag{A.8}$$

$$F_W + F_E = 0 \tag{A.9}$$

In the equilibrium equations (A.1)-(A.9) the term F_*^x is defined as the component of the force F_* in the horizontal direction and the term F_*^y as the components of the force F_* in the vertical direction. By solving the above equilibrium equations the reaction force F_E and the forces in the mechanism OCB can be determined as a function of the spring force F_A. This leads to the following relations between the forces acting on the mechanism OCB and the rigid frame CE and the spring force F_A.

$$F_O^x = -F_A \qquad F_B^x = -F_A \tag{A.10}$$

$$F_O^y = -F_A\frac{\sin\theta_1}{\cos\theta_1} \qquad F_B^y = -F_A\frac{\sin\theta_1}{\cos\theta_1} \tag{A.11}$$

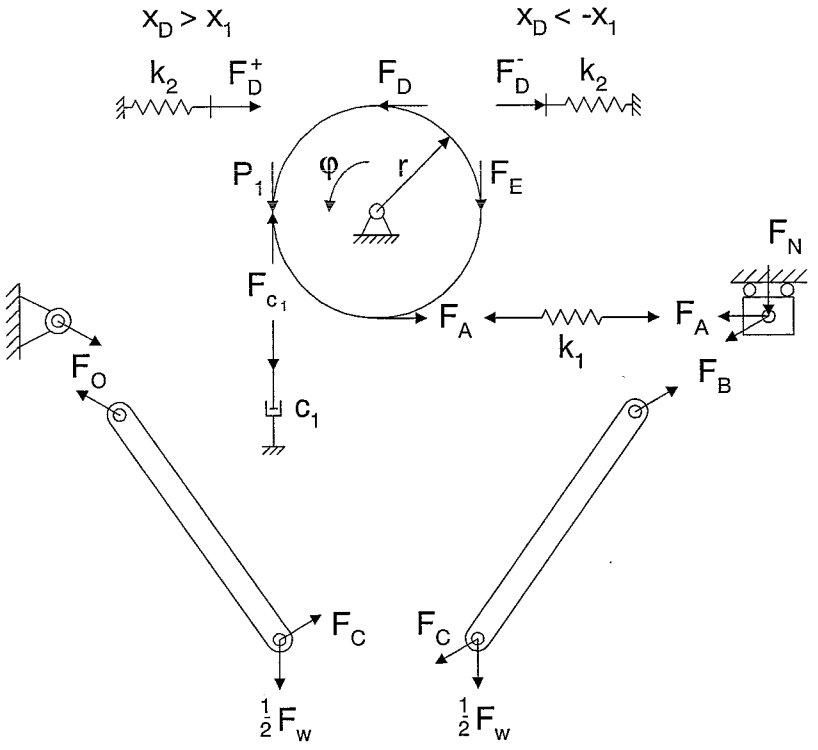

Figure A.1: The free body diagram of the mechanism that creates negative stiffness.

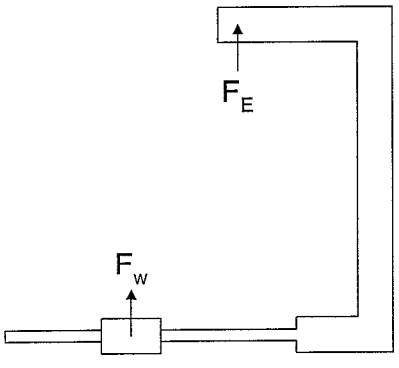

Figure A.2: A free body diagram of the rigid frame CE.

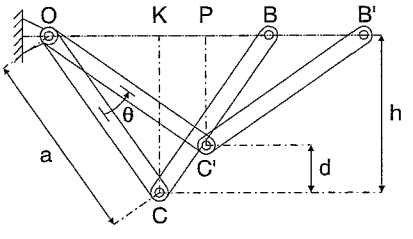

Figure A.3: A schematic drawing of the mechanism OCB.

$$F_C^x = -F_A \qquad F_N = F_A \frac{\sin\theta_1}{\cos\theta_1} \tag{A.12}$$

$$F_C^y = 0 \qquad F_W = -2\frac{\sin\theta_1}{\cos\theta_1} F_A \tag{A.13}$$

$$F_E = 2\frac{\sin\theta_1}{\cos\theta_1} F_A \tag{A.14}$$

The term $\frac{\sin\theta_1}{\cos\theta_1}$ can be determined from the kinematics of the mechanism OCB. Using figure A.3 the term $\frac{\sin\theta_1}{\cos\theta_1}$ can be written as:

$$\frac{\sin\theta_1}{\cos\theta_1} = \frac{PC'}{OC'} = \frac{h - r\sin\varphi}{\sqrt{a^2 - (h - r\sin\varphi)^2}} \tag{A.15}$$

Substituting the expression for the spring force F_A and equation (A.15) into equation (A.14) leads to the following expression for the reaction force F_E:

$$F_E = 2k_1 \left(\frac{2h}{\sqrt{a^2 - h^2}} - 1 \right) \left(\frac{h - r\sin\varphi}{\sqrt{a^2 - (h - r\sin\varphi)^2}} \right) r\varphi \tag{A.16}$$

This equation is clearly not equal to the definition for F_E found in [1]. By taking the geometric factor $\frac{\sin\theta_1}{\cos\theta_1}$ at $\varphi = 0$ equation (A.16) can be made almost identical to the expression found in [1]. This leads to the following expression for the reaction force F_E:

$$F_E = 2k_1 \left(\frac{2h}{\sqrt{a^2 - h^2}} - 1 \right) \left(\frac{h}{\sqrt{a^2 - h^2}} \right) r\varphi \tag{A.17}$$

The differences between the above equation and the expression for F_E found in [1] is a constant factor of -2. This factor -2 is the reason why the analysis of the mechanism in [1] allows the generation of a negative stiffness while according to the analysis performed in this report this is not possible.

B The Relation Between Negative Resistance And Mechanical Stiffness

An import aspect in the analysis of the mechanical Chua is the assumption that the negative stiffness created by the mechanical Chua is equivalent to the negative resistance in the electrical Chua. This equivalence is not immediately apparent because in conventional systems the mechanical equivalent of an electrical resistance is a mechanical damper. The equivalence between the electrical and mechanical Chua is based on the nondimensional governing equations of both systems. The idea is that although there is no direct relation between negative resistance and negative stiffness both systems have identical nondimensional governing equations. To identify the relation between negative resistance and negative stiffness the nondimensional governing equations of the electrical and mechanical systems have to be analysed. This analysis can be restricted to the nondimensional governing equations that contain the negative resistance and negative stiffness terms.
The dimensional governing equation (2.1) of the electrical Chua is transformed in a nondimensional form by applying the following scaling to the dimensional state variables.

$$x \equiv \frac{v_1}{E} \qquad y \equiv \frac{v_2}{E} \qquad \tau \equiv \frac{G}{C_2}t \tag{B.1}$$

This leads to the following nondimensional governing equation for the electrical Chua.

$$\frac{dx}{d\tau} = \frac{C_2}{C_1}\left(y - x - f(x)\right) \tag{B.2}$$

Where the nondimensional negative resistance $f(x)$ is of the following form:

$$f(x) = \begin{cases} \frac{G_b}{G}x + \frac{G_a - G_b}{G} & x \geq 1 \\ \frac{G_a}{G}x & |x| < 1 \\ \frac{G_b}{G}x + \frac{G_b - G_a}{G} & x \leq -1 \end{cases} \tag{B.3}$$

The nondimensional governing equations of the mechanical Chua are defined by equations (4.6), (4.7) and (4.8). Equation (4.6) can be written into the following form.

$$\frac{d\widetilde{\varphi}}{d\tau} = \frac{\lambda_1 y^*}{c_1 \omega r \varphi^*}\left(\widetilde{y} - \widetilde{\varphi} - f(\widetilde{\varphi})\right) \tag{B.4}$$

Where the function $f(\widetilde{\varphi})$ is defined as:

$$f(\widetilde{\varphi}) = \begin{cases} -\left(1 + \frac{(k_1\delta - k_2)r\varphi^*}{\lambda_1 y^*}\right) - \frac{k_2 r\varphi^*}{\lambda_1 y^*} & \widetilde{\varphi} \geq 1 \\ -\left(1 + \frac{k_1\delta r\varphi^*}{\lambda_1 y^*}\right) & |\widetilde{\varphi}| < 1 \\ -\left(1 + \frac{(k_1\delta - k_2)r\varphi^*}{\lambda_1 y^*}\right) + \frac{k_2 r\varphi^*}{\lambda_1 y^*} & \widetilde{\varphi} \leq -1 \end{cases} \tag{B.5}$$

If the electrical and mechanical systems are equivalent then the nondimensional governing equations of both systems are identical. Substituting the expressions for the mechanical parameters as defined by equations (4.13), (4.14) (4.15), (4.16) and (4.17) in the mechanical nondimensional constant $\frac{\lambda_1 y^*}{c_1 \omega r \varphi^*}$ shows that this constant is identical to $\frac{C_2}{C_1}$. This means that if the electrical and mechanical system are equivalent then the function $f(\widetilde{\varphi})$ must be the nondimensional mechanical equivalent of the nondimensional negative resistance $f(x)$. Comparing the expressions for $f(\widetilde{\varphi})$ and $f(x)$ as defined by equations (B.3) and (B.5) shows that there is indeed no direct relation between the negative resistance and the negative stiffness. The nondimensional mechanical equivalent of a nondimensional ńegative resistance is a combination of the stiffness k_1, the stiffness k_2, the geometrical constant δ, the radius r and the electromechanical constant λ_1.

Bibliography

[1] M.L. Calvisi J. Awrejcewicz.
Mechanical models of chua's circuit.
International Journal On Bifurcation And Chaos, 12(4):671–686, 2002.

[2] M.P. Kennedy.
Three steps to chaos - part ii: A chua's circuit primer.
IEEE Transactions On Circuits And Systems I, 40(10):657–674, October 1993.

[3] Robert L. Norton.
Design Of Machinery: An Introduction To The Synthesis and Analysis of Mechanisms And Machines.
MECHANICAL ENGINEERING SERIES. McGRAW-HILL INTERNATION EDITIONS, 1992.